Type IV pili interactions promote intercellular association and moderate swarming of *Pseudomonas aeruginosa*

Morgen E. Anyan[a], Aboutaleb Amiri[b], Cameron W. Harvey[c], Giordano Tierra[c,d], Nydia Morales-Soto[a,e], Callan M. Driscoll[a,e], Mark S. Alber[b,c,f,1], and Joshua D. Shrout[a,e,g,1]

Departments of [a]Civil and Environmental Engineering and Earth Sciences, [b]Physics, [c]Applied and Computational Mathematics and Statistics, and [g]Biological Sciences, and [e]Eck Institute for Global Health, University of Notre Dame, Notre Dame, IN 46556; [d]Mathematical Institute, Charles University, 18675 Prague, Czech Republic; and [f]Department of Medicine, Indiana University School of Medicine, Indianapolis, IN 46202

Edited by Caroline S. Harwood, University of Washington, Seattle, WA, and approved November 10, 2014 (received for review August 4, 2014)

Pseudomonas aeruginosa **is a ubiquitous bacterium that survives in many environments, including as an acute and chronic pathogen in humans. Substantial evidence shows that *P. aeruginosa* behavior is affected by its motility, and appendages known as flagella and type IV pili (TFP) are known to confer such motility. The role these appendages play when not facilitating motility or attachment, however, is unclear. Here we discern a passive intercellular role of TFP during flagellar-mediated swarming of *P. aeruginosa* that does not require TFP extension or retraction. We studied swarming at the cellular level using a combination of laboratory experiments and computational simulations to explain the resultant patterns of cells imaged from in vitro swarms. Namely, we used a computational model to simulate swarming and to probe for individual cell behavior that cannot currently be otherwise measured. Our simulations showed that TFP of swarming *P. aeruginosa* should be distributed all over the cell and that TFP–TFP interactions between cells should be a dominant mechanism that promotes cell–cell interaction, limits lone cell movement, and slows swarm expansion. This predicted physical mechanism involving TFP was confirmed in vitro using pairwise mixtures of strains with and without TFP where cells without TFP separate from cells with TFP. While TFP slow swarm expansion, we show in vitro that TFP help alter collective motion to avoid toxic compounds such as the antibiotic carbenicillin. Thus, TFP physically affect *P. aeruginosa* swarming by actively promoting cell–cell association and directional collective motion within motile groups to aid their survival.**

collective motion | biofilms | computational model | predictive simulations | self-organization

The bacterium *Pseudomonas aeruginosa* is a ubiquitous organism that is a known opportunistic pathogen, causing both chronic and acute infections in susceptible populations, including individuals with cystic fibrosis or burn wounds, or Intensive Care Unit patients (1). Among questions that remain unanswered for nonobligate pathogens like *P. aeruginosa* is how these bacteria initiate infections after entering the host from the environment. Given that *P. aeruginosa* is among many bacteria that grow as a biofilm during infection, there is a need to understand how individual cells coordinate in space with each other to colonize new surfaces and subsequently transition to stationary biofilms.

Many organisms coordinate their movement as a population, emerging as self-organized swarming groups. Even the untrained eye would note the coordinated swarming behavior of fish, birds, and insects. Many bacteria also exhibit collective motion by swarming over surfaces in a coordinated manner to move unimpeded at the same time (2–4). Our knowledge of the specific actions used by individual cells during collective motion is limited; the behavior of single cells within a dense population is difficult to discern experimentally. Previous attempts to study bacterial collective behavior have used computational models to test mechanisms hypothesized to influence collective motion, including directional reversals (5), slime deposition and chemoregulation (6), quorum sensing and surfactant production (7), and escape-and-pursuit response (8). Cell-to-cell alignment is an included feature of many of these computational models and an experimental measurement frequently used to characterize ordering of cells within populations (9, 10). For example, assumption of higher alignment among cells to improve collective motion in model simulations was crucial to recreation of the density wave propagating with the velocity of the experimentally observed traveling wave in *P. aeruginosa* swarms (7). However, it is not yet clear if groups of bacteria truly coordinate (e.g., align) over longer distances and time scales to swarm. Such investigation has been limited to *Escherichia coli*, for which patterns of coordination have only been shown over short distances (11).

Swarming is often considered to be a transition step before formation of stationary biofilm communities. For *P. aeruginosa*, it has been demonstrated that biofilm formation and swarming are inversely regulated by intracellular concentrations of cis(3′–5′)-cyclic-diguanylate-monophosphate (c-di-GMP). Low levels of c-di-GMP promote surface swarming, whereas elevated levels of c-di-GMP cue production of *P. aeruginosa* matrix polysaccharides and the initiation of a sessile biofilm (12, 13). The diguanylate cyclase WspR, for example, up-regulates Pel polysaccharide synthesis in a contact-dependent manner (14). However, the specific physical

Significance

The opportunistic pathogen *Pseudomonas aeruginosa* utilizes both its flagellum and type IV pili (TFP) to facilitate motility, attachment, and colonization. Surface motility such as swarming is thought to precede biofilm formation during infection. We combined laboratory and computational methods to probe the physical interactions of TFP during flagellar-mediated swarming and found that TFP of one cell strongly interact with TFP of other cells, which limits swarming expansion rate. Hence, wild-type *P. aeruginosa* use cell–cell physical interactions via their TFP to control self-organization within motile swarms. This collective mechanism of cell–cell coordination using TFP allows for moderation of swarming direction of individual cells and avoidance of a toxic environment.

Author contributions: M.E.A., A.A., C.W.H., M.S.A., and J.D.S. designed research; M.E.A., A.A., C.W.H., G.T., N.M.-S., and C.M.D. performed research; M.S.A. and J.D.S. contributed new reagents/analytic tools; M.E.A., A.A., C.W.H., G.T., M.S.A., and J.D.S. analyzed data; and M.E.A., A.A., C.W.H., M.S.A., and J.D.S. wrote the paper.

The authors declare no conflict of interest.

This article is a PNAS Direct Submission.

[1]To whom correspondence may be addressed. Email: Joshua.Shrout@nd.edu or malber@nd.edu.

This article contains supporting information online at www.pnas.org/lookup/suppl/doi:10.1073/pnas.1414661111/-/DCSupplemental.

interaction(s) between *P. aeruginosa* and surfaces (e.g., swarming substrates, surfaces of attachment, or other *P. aeruginosa* cells) have yet to be elucidated in specific detail.

Most motile bacteria use either flagella or type IV pili (TFP), but *P. aeruginosa* is one of few bacteria that possess both of these motile appendage types. *P. aeruginosa* TFP or flagella confer multiple motility modes in addition to swarming, including swimming, twitching, crawling, and walking (15–17); *P. aeruginosa* requires a functional flagellum to swarm (18, 19). Although the fastest swarming bacteria (i.e., species of *Vibrio* or *Proteus*) transition to a hyperflagellated state or can evolve as hyperflagellated mutants (20–23), for this study, we have investigated monoflagellated bacteria characteristic of *P. aeruginosa* swarming. Both TFP and flagella are important to *P. aeruginosa* biofilm formation (24) and mediate attachment to different surfaces, including eukaryotic epithelial cells (25). Previous research suggests that TFP do not lead to faster swarming. For example, *P. aeruginosa* mutants of TFP pilin genes *pilA*, *pilW*, *pilX*, or *pilY1* (rendering them TFP deficient) exhibit an increased swarming phenotype (19, 26, 27), and retraction-impaired mutations, such as *pilH*, exhibit decreased swarming (28). Thus, in this paper, we addressed the question, "What role do TFP play in swarming?" More specifically, we were interested in studying how TFP contribute to collective motion during (flagellar-mediated) swarming of *P. aeruginosa*. Although separate studies suggest a broader regulatory role for some TFP-associated genes (26, 27), we judged the increased swarming exhibited by select TFP mutants as allowing for the possibility of a physical role of TFP during swarming.

In this paper, we present evidence that *P. aeruginosa* promotes physical cell–cell interactions during swarming via their TFP to control their collective motion and limit lone cell movement in swarms. Because of the difficulty of specifically identifying the influence and dynamics of TFP upon swarming cells using a traditional experimental approach, we used a series of coordinated laboratory and computational experiments to study the physical influence of TFP among groups of *P. aeruginosa* cells. Using simulations, we showed that prior reports of improved swarming by *P. aeruginosa* TFP-deficient mutants can be caused by TFP-deficient cells displaying increased displacement compared with wild-type cells. We confirmed this prediction in vitro by showing that a TFP-deficient mutant could outcompete *P. aeruginosa* wild type in coculture experiments to reach the swarm edge first. We also infer from our experiments that TFP interact strongly with other TFP during swarming and conclude that *P. aeruginosa* initiates TFP-based community building within motile swarms. We show the benefit of TFP-mediated collective motion control by showing that wild-type, but not TFP-deficient, *P. aeruginosa* alters its swarming to avoid high concentrations of the antibiotic carbenicillin.

Results

TFP Affect Cell–Cell Arrangement During Swarming. Given the observation of our group and others that TFP-deficient *P. aeruginosa* strains exhibit a hyperswarming phenotype (19, 26, 27), we were interested in explaining the role of TFP during swarming. How do TFP participate during swarming if they do not increase cell motility and are not conferring attachment to surfaces? We studied *P. aeruginosa* wild-type and TFP mutants under conditions where TFP-deficient swarms expand five times faster than wild-type swarms (Table S1 and Movie S1), despite the fact that these strains produce the same levels of rhamnolipid (19) and show the same swimming (flagellar motility) speed (Table S1). We found that the presence of TFP affects the arrangement of cells at the advancing swarm edge (Fig. 1). Cells without TFP (Δ*pilA*) appear more systematically ordered than wild-type cells while hyperpiliated (Δ*pilU*) cells appear less ordered than wild-type cells. Inspection of cells in swarm tendrils (~1–2 mm toward the swarm center away from the swarm edge) shows a less-marked

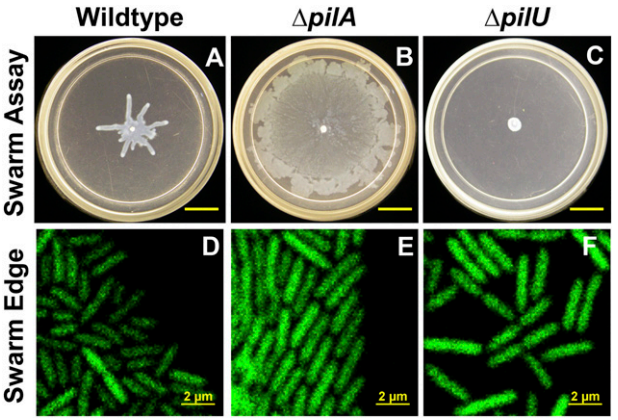

Fig. 1. Impact of TFP on *P. aeruginosa* swarming. (*A–C*) Whole population and (*D–F*) single-cell scales imaged by confocal microscopy during swarming of *P. aeruginosa* wild-type and isogenic Δ*pilA* (TFP-deficient) and Δ*pilU* (hyperpiliated) TFP mutants. The scale bars in *A–C* and *D–F* represent 12 mm and 2 μm, respectively.

distinction between cell–cell patterns for cells with and without TFP (Fig. S1).

We quantified these differences in arrangement between the TFP-deficient mutant and wild-type mutant by calculating the alignment, clustering, and density of cells identified in our confocal images. Alignment of cells was calculated by measuring the parallel orientation of each cell–cell pair identified in our confocal images (see *SI Materials and Methods* for details). Swarming cells without TFP exhibited the highest alignment values (Fig. 2*A*), but the same trends of alignment were observed for all strains. As expected, cell–cell pairs for all strains tested exhibited the greatest alignment with their closest neighbors (fewer than five cells apart). At greater distances, cell–cell alignment decreases for each different strain until reaching a constant alignment value. For cells that are away from the edges of these swarms (toward the swarm center), we find that wild-type cells exhibit roughly the same level of alignment within tendrils as at the swarm edge while TFP-deficient bacteria also converge to a less-aligned arrangement that is similar to wild type (for distances greater than one cell length) within these tendrils (Fig. S2*A*).

We also quantified cell–cell clustering and population density for swarming cells with and without TFP. We define a cluster as having cells with ≤15° difference in orientation and ≤3 μm separation (see *SI Materials and Methods* for details). The presence of TFP contributed to cluster size, as TFP-deficient cells were the most likely to form larger clusters of 10 or more cells (Fig. 3*A* and Fig. S2*B*), while hyperpiliated cells were more likely to exist as single cells. The majority of cells are not part of a cluster for any strain examined (i.e., cluster size is one cell). We also calculated population density as a packing fraction of cells within the available total space (i.e., cell coverage area divided by total swarm area—see *SI Materials and Methods* for details)—a higher packing fraction indicates that cells are more tightly packed. TFP-producing wild-type cells exhibited a packing fraction that is 60% of the TFP-deficient Δ*pilA* strain at their swarm edges (Table S1). Within these high-population swarms, TFP of wild-type cells appear to limit the 2D cell density that can be achieved for *P. aeruginosa*.

The influence of TFP upon swarming extends in all three dimensions, as we also noted differences in swarm profile height. *P. aeruginosa* TFP promote development of swarms with more height, or layers, of cells. By inspecting the *z* profile from confocal images of swarming cells, we were able to directly measure the height of these swarms along a radial axis from the swarm

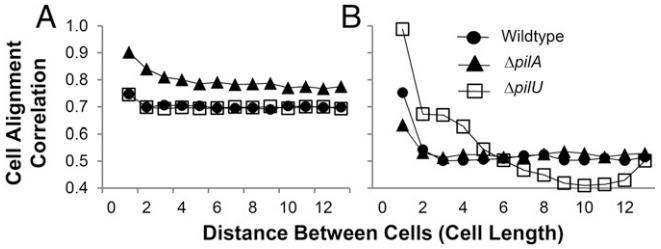

Fig. 2. Cell–cell alignment for swarm edge cells for wild-type and Δ*pilA* (TFP-deficient) swarms. The *y* axis values of 0–1 represent a measure of alignment where 1.0 = perfectly parallel cells, while 0 = perfectly perpendicular cells. The *x* axis values represent the number of cell lengths between the compared cells for (*A*) in vitro swarms calculated from images of swarming bacteria at the swarm edge obtained using confocal microscopy similar to Fig. 1 *D* and *E* (for six images containing 122–715 cells each) and (*B*) in silico computational simulation results of swarming bacteria.

center to the swarm edge. Profile measurements of wild-type and Δ*pilA* swarms indicated that TFP promoted taller swarming communities (Fig. S3); the average height along the swarm radius of wild type was roughly double that of TFP-deficient cells (Table S1). The shorter height of TFP-deficient swarm tendrils is likely explained by improved spreading, as the TFP-deficient strain swarmed 7 mm farther, on average, than wild type. The height profile for swarms of all strains decreases dramatically toward their advancing edge, eventually thinning to a monolayer of cells.

Simulations of Swarming Cells Predict That TFP Affect Collective Motion. Because of the difficulty of specifically identifying the role of TFP for single cells during swarming using a traditional laboratory approach, we examined a potential TFP interaction mechanism among cells using computational modeling (in silico). A cell-based computational model of *P. aeruginosa* motion and interaction was used where TFP, distributed uniformly around a cell, affect cell trajectory and turning but not self-propulsion of the cell (see *SI Materials and Methods* for details and Fig. S4 for a schematic depicting the basics of this interaction). The model was calibrated using experimental data obtained at different scales for individual *P. aeruginosa* cells and entire *P. aeruginosa* swarms. Simulation experiments were then conducted using this model to study the importance of specific cellular attributes to collective motion of swarming where we could simulate and track the behavior of every cell over time as well as collective behavior of the population.

We observed differences between TFP and non-TFP strains in our simulations, but were unable to capture the emerging arrangement patterns seen and measured in our swarm plate assays. Altering the range (or zone) of TFP interaction did not lead to the emerging cell alignment or clustering measured in vitro. For example, the level of alignment in our simulations differed between wild-type, TFP-deficient, and hyperpiliated strains at short range distances (Fig. 2*B*). Additionally, simulated swarming cells also did not converge to a minimum alignment as observed in vitro.

With regard to clustering, the simulations partially captured the clustering phenotypes observed in vitro (Fig. 3*B*). The simulation results did fit the general pattern observed for wild-type cells with TFP; however, the absence of TFP did not lead to the greater cluster sizes observed in vitro (Fig. 3). Overall, the differences in alignment and clustering between these in vitro and in silico experiments suggest that these cell–cell arrangement properties are not causative traits for differences in collective motion of bacteria. Hence, if our assumption that TFP impact cell–cell motion is correct, the faster collective motion of TFP-deficient cells must involve cell–cell interactions that promote more than just parallel cell alignment and cluster size to affect swarming. Since few flagellar-motile bacteria also have functional TFP, it is possible that traits of collective motion exhibited by *P. aeruginosa* to swarm are distinct from those of other bacterial species. Although some subclassification to distinguish different swarming bacteria has been introduced (4), it may be further advantageous to specifically distinguish the collective motion traits of swarming bacteria to build upon the original definition of Henrichsen (29).

We further analyzed our in silico results to determine how populations with and without TFP might swarm differently. We calculated the mean squared displacement (MSD) over time for simulations of cells with and without TFP, and found that the population of cells exhibited three different types of behavior that can be separated into phases (or regimes) that have been studied for small self-propelled particles (see *SI Materials and Methods* for details) (30–32). The MSD for wild-type cells with TFP was much less than for TFP-deficient cells (Fig. 4*A*). We also implemented TFP–TFP interaction among swarming bacteria in a probabilistic manner to consider the possibility that TFP between neighboring cells may not always interact. Our simulations showed that decreasing the probability that TFP interact between neighboring cells leads to increased swarm expansion and MSD of these cells (Fig. 4*B*). Thus, our in silico results predicted that *P. aeruginosa* cells that have minimal TFP–TFP interaction or cells without TFP should spread more easily (as individual cells) than wild-type cells with considerable TFP interaction at any time during swarm expansion. We also considered the possible placement of TFP on swarming cells by simulating cells with TFP present on only half of the cell rod and only at one cell pole. We found that TFP placement also impacts swarm expansion, as cells with more polar TFP exhibited greater swarm expansion and MSD values (Fig. 4*C*). Lastly, we simulated swarming for a mixture of cells with and without TFP and again find that the MSD of cells without TFP is greater than cells with TFP (Fig. 4*D*). We therefore conclude from these in silico results that increasing parallel alignment does not improve collective motion a priori; rather, cells within swarms that expand faster tend to exhibit higher alignment. These changes in displacement did not have a linear correlation with alignment or clustering of these cells. Although previous research has postulated that *P. aeruginosa* cells must align with each other to allow swarms to expand in some cases (4, 7), our results suggest alignment as a consequence of swarming behavior rather than

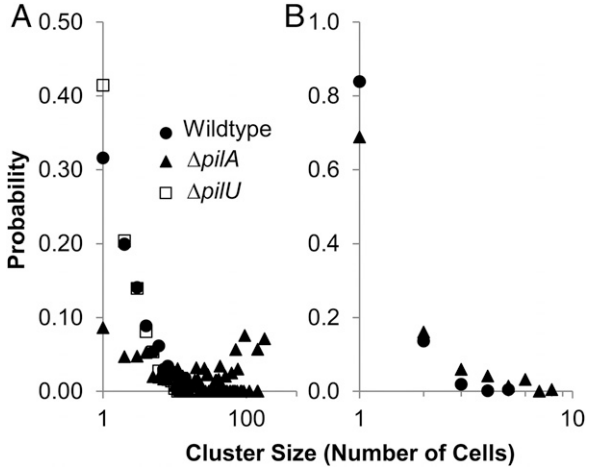

Fig. 3. Cell clustering during swarming. Cluster size distribution for (*A*) in vitro swarm edge cells ($n \geq 122$ frames), where TFP-deficient cells are more likely to form large clusters (>10 cells) than wild-type cells at the swarm edge, and (*B*) in silico simulations.

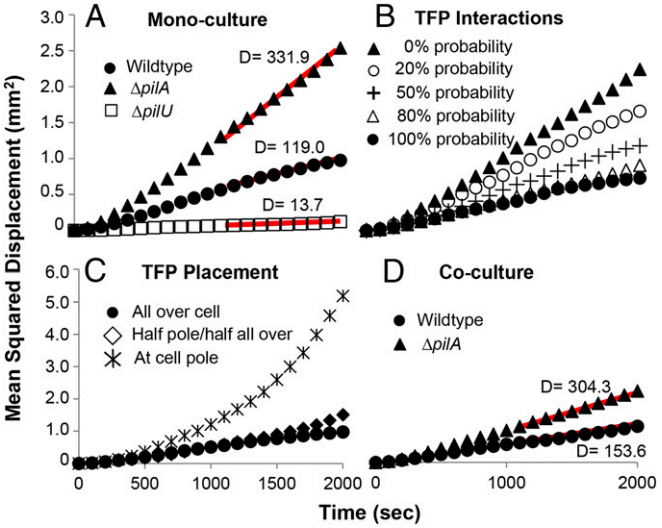

Fig. 4. Computational simulations of swarming bacteria show MSD of cells over time to be impacted by TFP. The effective cell density of each simulation was kept constant at 75%. (*A*) Monocultures simulated with differing amounts of TFP. TFP-deficient cells are modeled as having no TFP, whereas wild-type cells have 0.5-μm-long TFP and hyperpiliated cells have 1.0-μm-long TFP. (*B*) Monoculture of wild-type cells with varied probability of TFP–TFP interaction. (*C*) Monoculture of cells with varied TFP placement. (*D*) Coculture simulation of wild-type with TFP-deficient cells that assumes only TFP–TFP interactions and no TFP–cell interactions. The total number of cells in this simulation was 360, and they were randomly assigned to be either TFP deficient or wild type at the onset of the simulation. The MSD coefficient D ($\mu m^2/s$) for cells in *A* and *D* is measured by linear fit data within the diffusive phase indicated by the red line.

a conditional requirement for *P. aeruginosa*. We attributed the higher expansion rates of TFP-deficient strains observed in vitro with increases in MSD rate when limiting TFP–TFP interactions between cells within motile populations.

TFP Interact with Other TFP During Swarming. To test our simulation prediction that single bacteria with or without TFP should spread differently within swarms, we conducted in vitro experiments with cocultures of *P. aeruginosa* strains with and without TFP. We found that cells with TFP largely interacted with other TFP-producing cells. Swarms composed of a 1:1 ratio of wild-type and Δ*pilA* cells exhibit a swarm phenotype that appears between that of wild-type and TFP-deficient swarms (Fig. 5). Swarms composed of a 1:10 ratio of Δ*pilA* cells and wild-type cells exhibit an overall pattern that is similar to the wild type alone. However, inspection of single cells within these coculture swarms shows that these strains are not uniformly distributed. At either inoculation ratio, coculture swarm edges become dominated by TFP-deficient cells, while swarm centers are almost exclusively populated by wild-type cells. When wild-type and TFP-deficient cells are present in roughly equal numbers, TFP-deficient cells concentrate on top of the wild-type cells (Fig. S5*B*). In all dimensions, interaction between cells with and without TFP appears limited. Overall, TFP-deficient cells advance more rapidly than wild type when growing in coculture (Movie S1). Further, we find these differences in swarm expansion are general for mixing any two strains with differing levels of TFP. For pairwise mixtures of TFP-deficient, wild-type, and hyperpiliated strains examined in vitro, the Δ*pilA* TFP-deficient strain always expands the fastest, the wild type has the next highest expansion rate, and the Δ*pilU* hyperpiliated strain has the slowest swarm expansion rate. Fig. S6 shows the phenotype of these different swarm mixtures and the distribution of cells at the swarm edge. Similarly, the strain with fewer TFP always localizes to the top of the swarm (Fig. S5). This consistent separation between cell types suggests that TFP are important to interactions among *P. aeruginosa* cells during swarming. In coculture these TFP-deficient cells exhibit a higher diffusivity than their TFP-producing counterparts. Because wild-type cells do not cluster with TFP-deficient cells to improve their spreading, we conclude that wild-type cells display strong associations by their TFP, thus excluding the TFP-deficient cells.

We then tested possible physical mechanisms for these observations using additional computational simulations that examined cells with and without TFP interacting in the same space. When TFP-deficient cells were introduced to a population of cells with TFP in a simulation, they were able to move through this population of TFP cells (Movie S2). Conversely, motile cells with TFP moved in clusters and not as single cells. The TFP-deficient cells in these simulations traveled farther and more of these cells reached the swarm edge than motile cells with TFP (Fig. S6). Thus, we explain the reduced spreading rate of wild-type compared with TFP-deficient cells as caused by TFP interacting primarily, if not solely, with other TFP during swarming. The ability of TFP-deficient cells to pass through wild-type (TFP-joined) cell clusters was then observed experimentally when inspecting swarming cells for a few seconds roughly 10 h after inoculation (Movie S3). While wild-type cells were not static, we show a representative example where wild-type cells remained associated with each other while TFP-deficient cells moved past wild type to reach the swarm edge in a manner similar to that predicted in our computational simulations.

Lastly, we demonstrated a benefit of TFP during swarming by monitoring growth of the wild-type and TFP-deficient strains in the presence of a toxic agent. In plate assays where we spotted a solution containing the β-lactam antibiotic carbenicillin, we observed that wild-type cells avoid this region of the plate (Fig. 6). Similar results showing *P. aeruginosa* swarms avoiding various inhibitory compounds have been shown in other studies (33, 34). Conversely, the TFP-deficient Δ*pilA* mutant swarmed at its higher expansion rate and proceeded into the region containing the highest amounts of antibiotic. The stress to cells exposed to carbenicillin diffusing away from the point of addition was readily apparent for both wild type and Δ*pilA* at the edges of these swarms, as exhibited by their elongation (Fig. 6 *D* and *H*). Within the timeframe of the experiment (~19 h), viability staining showed many of these cells stain "dead" by propidium iodide. However, the uncontrolled TFP-deficient cells exhibited amplified signs of their exposure to carbenicillin for much of its swarm area. The TFP-deficient swarms showed cell elongation

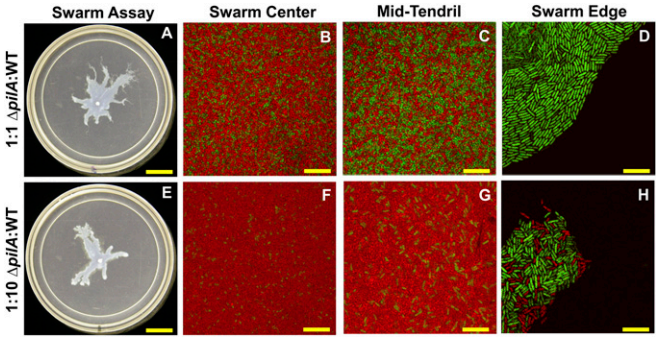

Fig. 5. Wild-type (WT) cells (red) do not prevent expansion of TFP-deficient (Δ*pilA*) (green) cells in coculture swarms. TFP-deficient cells do not colocalize with WT over time and are most prevalent at the edges of cocultured swarms, while WT cells dominate the swarm center. This phenotype is observed at inoculation ratios of either (*A–D*) 1:1 or (*E–H*) 1:10 Δ*pilA*:WT. The scale bars for *A* and *E* represent 10 mm, and the scale bars for *B–D* and *F–H* represent 2 μm.

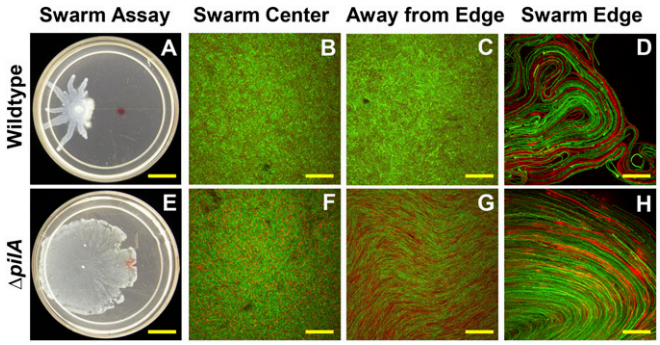

Fig. 6. TFP limit expansion to allow for avoiding toxic environments during swarming. (*A*) *P. aeruginosa* wild type avoids a spot inoculation of 63 μg carbenicillin (marked by red dot). (*E*) The isogenic Δ*pilA* (TFP-deficient) strain swarms over the carbenicillin. (*B–D* and *F–H*) Single-cell scale of swarms imaged by confocal microscopy. Cell elongation and cell death (i.e., stained red with propidium iodide) is apparent in maximum-intensity projections of confocal micrographs at the edges for both (*D*) wild type and (*H*) Δ*pilA*. The impact of carbenicillin is more widespread for the (*G*) Δ*pilA*, as exampled ∼25 mm from its swarm edge, compared with (*C*) wild type ∼4 mm from the swarm edge. The scale bars for *A* and *E* represent 10 mm, and the scale bars for *B–D* and *F–H* represent 20 μm.

and cell death well away from their advancing swarm edge. Hence, the TFP–TFP associations that reduced overall swarming allowed *P. aeruginosa* cell groups to deviate their overall swarming direction to avoid a toxic environment.

Discussion

We conclude that *P. aeruginosa* TFP preferentially interact with TFP of other cells during swarming to promote cell–cell association and limit lone cell movement in expanding swarms. We reached this conclusion by studying swarming of *P. aeruginosa* wild-type and TFP-mutant strains using computational simulation (in silico) experiments and in vitro plate assay swarming experiments in an iterative fashion. We first detailed differences in cell–cell patterning during swarming for cells with and without TFP from in vitro experiments (Fig. 1). We then explored potential mechanism of TFP interactions between cells using a cell-based computational model to simulate *P. aeruginosa* swarming. Our simulation results predicted that displacement properties of single cells should be affected by TFP. Additional simulations predicted that mixtures of cells with and without TFP should separate. We confirmed the in silico predictions of displacement and separation behavior by showing in vitro that TFP-deficient cells will predominate at swarm edges in co-culture swarm experiments, even when added 1:10 with a wild-type strain harboring more TFP (Fig. 5 and Movie S1). Not only did the TFP-deficient (Δ*pilA*) strain spread faster during swarming, but this strain also consistently separated from the TFP-producing wild type. Thus, we infer that TFP–TFP interactions between *P. aeruginosa* cells are a dominant mechanism of cell–cell interaction during swarming. This mechanism was general for *P. aeruginosa* strains with differing TFP levels, as groups of strains with more TFP could always be distinguished from strains with fewer (or no) TFP over time in our experiments (Fig. S6).

The TFP–TFP interactions we report help explain previous experimental results that showed increased swarming of TFP-deficient mutant strains (19, 26, 27) even though the (uninhibited) swim motility of these strains is the same (Table S1). Effectively, wild-type *P. aeruginosa* limit their collective motion because of TFP interactions. The importance of TFP associations for *P. aeruginosa* communities for development of static biofilms is well established (35–37). Here we further extend our knowledge of TFP function by demonstrating that TFP allow swarming *P. aeruginosa* some directional control of its collective motion. The direct advantage of this TFP mechanism during swarming was evidenced when swarms are monitored in the presence of the antibiotic carbenicillin. A TFP-deficient strain was unable to alter its radial swarming direction and traveled into a toxic environment that led to cell death (Fig. 6). TFP-intact wild-type cells were able to stop swarming in the direction of this soluble toxic compound, thus promoting their survival.

Based upon our in silico and in vitro results, we conclude that the TFP influence upon collective behavior we report is passive and does not require extension and retraction of TFP. No displacement of cells could be discerned that would be consistent with TFP retraction (Movie S3). Our simulations were able to capture the results we observed in vitro when we assumed a high interaction probability between cells with uniformly distributed TFP. These results are also consistent with a nonretraction TFP mechanism, as *P. aeruginosa* cells displaying TFP-mediated motility are reported to have polar TFP (38, 39).

The duration of the TFP–TFP/cell–cell associations we report remains to be determined. TFP associations as a precursor to biofilm formation have been observed for *Vibrio cholerae* (40). Here, *P. aeruginosa* may be using TFP as a means of sensing physical proximity to neighbor cells in addition to sensing population density via diffusible quorum sensing cues. Such a mechanism is in agreement with evidence showing swarming as a transition step between initial surface colonization and static biofilm development (15, 19, 27, 37, 41). Further evidence for this transitional role for swarming was provided by van Ditmarsch et al., who demonstrated that selection for hyperswarming *P. aeruginosa* mutations comes at a fitness cost, as these mutants were at a disadvantage in other phenotypic assays (42). Importantly, none of the hyperswarming mutants obtained by van Ditmarsch et al. were TFP deficient. Evolving to curtail TFP synthesis must come at a cost even for swarming *P. aeruginosa* even in the absence of an antagonist, as we have demonstrated in our experiments. We suggest that this can be explained by the ability of TFP to confer advantageous cell–cell associations by linking to other TFP.

Materials and Methods

Bacterial Strains and Culturing Conditions. All strains and plasmids used in this study are included in Table S2, and culturing conditions are detailed in *SI Materials and Methods*.

Swarm Assays. Swarm motility plate assays contained fastidious anaerobe broth-casamino acids minimal media solidified with 0.45% Noble agar (Sigma) and were inoculated with planktonic cultures as described in *SI Materials and Methods*.

Microscopy and Imaging. Images of swarming bacteria expressing GFP or mCherry were obtained using confocal microscopy and entire swarms were imaged using a Carestream multispectral FX or In-Vivo Xtreme imaging station as described previously (3). Specific detail is provided in *SI Materials and Methods*.

Analysis of Patterning in Experimental Images. Representative images of swarm edges and swarm tendrils were analyzed using a cell alignment and cluster algorithm (*SI Materials and Methods*). Calculated values from this analysis were also used to compute average cell lengths and packing fraction of groups of cells.

Construction and Complementation of New Mutants. All strains used in this study were constructed previously (Table S2), with the exceptions of the wild-type-mCherry, Δ*pilU*, Δ*pilU*-GFP, and Δ*fliM*Δ*pilA*-GFP mutants (*SI Materials and Methods*).

Computational Simulation of *P. aeruginosa* Swarming. TFP have a polymer structure and show complex behavior under external forces. Cells linked together via TFP can behave similarly to cross-linked networks such as liquid crystals. In our model, we approximate TFP–TFP interaction with a linear force

as for a spring, which is based on prior investigation of pili of *E. coli* and *P. aeruginosa* (43–45). Cells were modeled as rigid capsule having an external TFP zone with a relaxed length equal to the average length of pili. As the cells get closer than the set cutoff distance (twice the pili length), the spring becomes compressed and a repulsion force and torque arises between the cells. The force pushes cells apart and the torque changes their orientations. (Additional details of our modeling approach are provided in *SI Materials and Methods*.)

ACKNOWLEDGMENTS. We thank Matthew Leevy of the Notre Dame Integrated Imaging Facility for imaging assistance. We thank Igor Aranson of Argonne National Laboratory for helpful discussion on physics of particle motion. This research was supported by funding from National Institutes of Health (NIH) Grant 1R01GM095959-01A1 (to M.S.A. and J.D.S.) and a Core Facility grant from the Indiana Clinical and Translational Sciences Institute (funded in part by NIH Grant UL1 TR000006) (to J.D.S.).

1. Gaynes R, Edwards JR; National Nosocomial Infections Surveillance System (2005) Overview of nosocomial infections caused by gram-negative bacilli. *Clin Infect Dis* 41(6):848–854.
2. Köhler T, Curty LK, Barja F, van Delden C, Pechère JC (2000) Swarming of *Pseudomonas aeruginosa* is dependent on cell-to-cell signaling and requires flagella and pili. *J Bacteriol* 182(21):5990–5996.
3. Morris JD, et al. (2011) Imaging and analysis of *Pseudomonas aeruginosa* swarming and rhamnolipid production. *Appl Environ Microbiol* 77(23):8310–8317.
4. Partridge JD, Harshey RM (2013) Swarming: Flexible roaming plans. *J Bacteriol* 195(5): 909–918.
5. Wu Y, Kaiser AD, Jiang Y, Alber MS (2009) Periodic reversal of direction allows Myxobacteria to swarm. *Proc Natl Acad Sci USA* 106(4):1222–1227.
6. Czirók A, Ben-Jacob E, Cohen I, Vicsek T (1996) Formation of complex bacterial colonies via self-generated vortices. *Phys Rev E Stat Phys Plasmas Fluids Relat Interdiscip Topics* 54(2):1791–1801.
7. Du H, et al. (2012) High density waves of the bacterium *Pseudomonas aeruginosa* in propagating swarms result in efficient colonization of surfaces. *Biophys J* 103(3): 601–609.
8. Romanczuk P, Couzin ID, Schimansky-Geier L (2009) Collective motion due to individual escape and pursuit response. *Phys Rev Lett* 102(1):010602.
9. Pelling AE, et al. (2006) Self-organized and highly ordered domain structures within swarms of *Myxococcus xanthus*. *Cell Motil Cytoskeleton* 63(3):141–148.
10. Zhang HP, Be'er A, Florin E-L, Swinney HL (2010) Collective motion and density fluctuations in bacterial colonies. *Proc Natl Acad Sci USA* 107(31):13626–13630.
11. Darnton NC, Turner L, Rojevsky S, Berg HC (2010) Dynamics of bacterial swarming. *Biophys J* 98(10):2082–2090.
12. Kuchma SL, et al. (2007) BifA, a cyclic-Di-GMP phosphodiesterase, inversely regulates biofilm formation and swarming motility by *Pseudomonas aeruginosa* PA14. *J Bacteriol* 189(22):8165–8178.
13. Hickman JW, Harwood CS (2008) Identification of FleQ from *Pseudomonas aeruginosa* as a c-di-GMP-responsive transcription factor. *Mol Microbiol* 69(2):376–389.
14. Huangyutitham V, Güvener ZT, Harwood CS (2013) Subcellular clustering of the phosphorylated WspR response regulator protein stimulates its diguanylate cyclase activity. *MBio* 4(3):e00242-13.
15. Burrows LL (2012) *Pseudomonas aeruginosa* twitching motility: Type IV pili in action. *Annu Rev Microbiol* 66:493–520.
16. Conrad JC, et al. (2011) Flagella and pili-mediated near-surface single-cell motility mechanisms in *P. aeruginosa*. *Biophys J* 100(7):1608–1616.
17. Gibiansky ML, et al. (2010) Bacteria use type IV pili to walk upright and detach from surfaces. *Science* 330(6001):197.
18. Caiazza NC, Shanks RMQ, O'Toole GA (2005) Rhamnolipids modulate swarming motility patterns of *Pseudomonas aeruginosa*. *J Bacteriol* 187(21):7351–7361.
19. Shrout JD, et al. (2006) The impact of quorum sensing and swarming motility on *Pseudomonas aeruginosa* biofilm formation is nutritionally conditional. *Mol Microbiol* 62(5):1264–1277.
20. Be'er A, Strain SK, Hernández RA, Ben-Jacob E, Florin E-L (2013) Periodic reversals in *Paenibacillus dendritiformis* swarming. *J Bacteriol* 195(12):2709–2717.
21. Morgenstein RM, Szostek B, Rather PN (2010) Regulation of gene expression during swarmer cell differentiation in *Proteus mirabilis*. *FEMS Microbiol Rev* 34(5):753–763.
22. Gode-Potratz CJ, Kustusch RJ, Breheny PJ, Weiss DS, McCarter LL (2011) Surface sensing in *Vibrio parahaemolyticus* triggers a programme of gene expression that promotes colonization and virulence. *Mol Microbiol* 79(1):240–263.
23. Deforet M, van Ditmarsch D, Carmona-Fontaine C, Xavier JB (2014) Hyperswarming adaptations in a bacterium improve collective motility without enhancing single cell motility. *Soft Matter* 10(14):2405–2413.
24. O'Toole GA, Kolter R (1998) Flagellar and twitching motility are necessary for *Pseudomonas aeruginosa* biofilm development. *Mol Microbiol* 30(2):295–304.
25. Bucior I, Pielage JF, Engel JN (2012) *Pseudomonas aeruginosa* pili and flagella mediate distinct binding and signaling events at the apical and basolateral surface of airway epithelium. *PLoS Pathog* 8(4):e1002616.
26. Kuchma SL, Griffin EF, O'Toole GA (2012) Minor pilins of the type IV pilus system participate in the negative regulation of swarming motility. *J Bacteriol* 194(19): 5388–5403.
27. Kuchma SL, et al. (2010) Cyclic-di-GMP-mediated repression of swarming motility by *Pseudomonas aeruginosa*: The *pilY*1 gene and its impact on surface-associated behaviors. *J Bacteriol* 192(12):2950–2964.
28. Yeung ATY, et al. (2009) Swarming of *Pseudomonas aeruginosa* is controlled by a broad spectrum of transcriptional regulators, including MetR. *J Bacteriol* 191(18): 5592–5602.
29. Henrichsen J (1972) Bacterial surface translocation: A survey and a classification. *Bacteriol Rev* 36(4):478–503.
30. Huang R, et al. (2011) Direct observation of the full transition from ballistic to diffusive Brownian motion in a liquid. *Nat Phys* 7(7):576–580.
31. Dhar P, et al. (2006) Autonomously moving nanorods at a viscous interface. *Nano Lett* 6(1):66–72.
32. Rafaï S, Jibuti L, Peyla P (2010) Effective viscosity of microswimmer suspensions. *Phys Rev Lett* 104(9):098102.
33. Bernier SP, Ha D-G, Khan W, Merritt JH, O'Toole GA (2011) Modulation of *Pseudomonas aeruginosa* surface-associated group behaviors by individual amino acids through c-di-GMP signaling. *Res Microbiol* 162(7):680–688.
34. Lai S, Tremblay J, Déziel E (2009) Swarming motility: A multicellular behaviour conferring antimicrobial resistance. *Environ Microbiol* 11(1):126–136.
35. Klausen M, et al. (2003) Biofilm formation by *Pseudomonas aeruginosa* wild type, flagella and type IV pili mutants. *Mol Microbiol* 48(6):1511–1524.
36. Klausen M, Aaes-Jørgensen A, Molin S, Tolker-Nielsen T (2003) Involvement of bacterial migration in the development of complex multicellular structures in *Pseudomonas aeruginosa* biofilms. *Mol Microbiol* 50(1):61–68.
37. Barken KB, et al. (2008) Roles of type IV pili, flagellum-mediated motility and extracellular DNA in the formation of mature multicellular structures in *Pseudomonas aeruginosa* biofilms. *Environ Microbiol* 10(9):2331–2343.
38. Skerker JM, Berg HC (2001) Direct observation of extension and retraction of type IV pili. *Proc Natl Acad Sci USA* 98(12):6901–6904.
39. Chiang P, et al. (2008) Functional role of conserved residues in the characteristic secretion NTPase motifs of the *Pseudomonas aeruginosa* type IV pilus motor proteins PilB, PilT and PilU. *Microbiology* 154(Pt 1):114–126.
40. Jude BA, Taylor RK (2011) The physical basis of type 4 pilus-mediated microcolony formation by *Vibrio cholerae* O1. *J Struct Biol* 175(1):1–9.
41. Caiazza NC, Merritt JH, Brothers KM, O'Toole GA (2007) Inverse regulation of biofilm formation and swarming motility by *Pseudomonas aeruginosa* PA14. *J Bacteriol* 189(9):3603–3612.
42. van Ditmarsch D, et al. (2013) Convergent evolution of hyperswarming leads to impaired biofilm formation in pathogenic bacteria. *Cell Reports* 4(4):697–708.
43. Jass J, et al. (2004) Physical properties of *Escherichia coli* P pili measured by optical tweezers. *Biophys J* 87(6):4271–4283.
44. Andersson M, Axner O, Almqvist F, Uhlin BE, Fällman E (2008) Physical properties of biopolymers assessed by optical tweezers: Analysis of folding and refolding of bacterial pili. *ChemPhysChem* 9(2):221–235.
45. Touhami A, Jericho MH, Boyd JM, Beveridge TJ (2006) Nanoscale characterization and determination of adhesion forces of *Pseudomonas aeruginosa* pili by using atomic force microscopy. *J Bacteriol* 188(2):370–377.